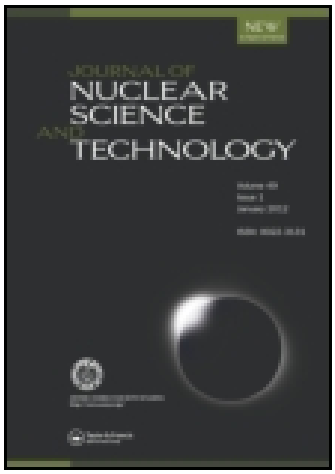

Journal of Nuclear Science and Technology
Publication details, including instructions for authors and subscription information:
http://www.tandfonline.com/loi/tnst20

Estimation of release rate of iodine-131 and cesium-137 from the Fukushima Daiichi nuclear power plant

Shigekazu Hirao [a] , Hiromi Yamazawa [a] & Takuya Nagae [a]
[a] Department of Energy Engineering and Science, Graduate School of Engineering , Nagoya University, Furo-cho, Chikusa-ku , Nagoya , 464-8603 , Japan
Published online: 28 Jan 2013.

To cite this article: Shigekazu Hirao , Hiromi Yamazawa & Takuya Nagae (2013) Estimation of release rate of iodine-131 and cesium-137 from the Fukushima Daiichi nuclear power plant, Journal of Nuclear Science and Technology, 50:2, 139-147, DOI: 10.1080/00223131.2013.757454

To link to this article: http://dx.doi.org/10.1080/00223131.2013.757454

Journal of Nuclear Science and Technology, 2013
Volume 50, No. 2, 139–147, http://dx.doi.org/10.1080/00223131.2013.757454

Taylor & Francis
Taylor & Francis Group

ARTICLE *Fukushima NPP Accident Related*

Estimation of release rate of iodine-131 and cesium-137 from the Fukushima Daiichi nuclear power plant

Shigekazu Hirao*, Hiromi Yamazawa and Takuya Nagae

Department of Energy Engineering and Science, Graduate School of Engineering, Nagoya University, Furo-cho, Chikusa-ku, Nagoya 464-8603, Japan

(*Received 22 October 2012; accepted final version for publication 30 November 2012*)

The atmospheric release rates of I-131 and Cs-137 from the Fukushima Daiichi nuclear power plant in March 2011 were estimated by comparing environmental monitoring data of air concentration and deposition rate on a regional scale with calculated values from an atmospheric dispersion model. Although the release rates were not estimated for all days after 11 March, because of lack of monitoring data, temporal changes in the release rates were reasonably estimated with estimated uncertainties in a factor of 3.3 and 2.9 for I-131 and Cs-137, respectively. A large release was estimated from the night of 14 March to at least the afternoon of 15 March, with maximum values of 7.2×10^{15} Bq h^{-1} for I-131 and 1.5×10^{14} Bq h^{-1} for Cs-137. The release rates during other periods were estimated at one- to two-orders of magnitude smaller than the largest release rate on 15 March. Uncertainty in the estimated release rate for 15 and 20 March was larger than for other periods. The significant release during 14 and 15 March and the trend of the release rate by the end of March were consistent with previous reports. This agreement, despite using different datasets, shows robustness of the temporal changes estimated in the studies.

Keywords: release rate estimation; Fukushima Daiichi nuclear power plant accident; atmospheric dispersion model; air concentration; deposition rate; regional scale

1. Introduction

A significant number of radionuclides were discharged into the environment from the Fukushima Daiichi nuclear power plant (FDNPP) on the eastern coast of Honshu Island in Japan as a result of the accident of Units 1–3 caused by the disabling of the reactor cooling systems owing to the 2011 earthquake off the Pacific coast of Tohoku and the subsequent tsunami. To evaluate public exposure to the radionuclides, estimates of the number of radionuclides released are urgently required.

The total amount of I-131 and Cs-137 released from FDNPP into the atmosphere have been estimated to be in the range of $(1.2–3.8) \times 10^{17}$ Bq and $(0.6–5.3) \times 10^{16}$ Bq, respectively [1–8]. From the standard deviation of these data, an uncertainty of 60%–90% is estimated in these results. Although the uncertainty in the accumulated release amount seems to be small, the uncertainty in the temporal change of release rate is expected to be fairly large.

To understand the processes of atmospheric dispersion and deposition of the radionuclides on a ground, the temporal change in the release rate is necessary. Several studies have estimated the temporal change by combining atmospheric dispersion simulations and environmental monitoring data [1–4,8,9]. These studies unanimously concluded that the atmospheric release of radionuclides began in the morning of 12 March when the air dose rate at the monitoring posts near FDNPP increased. The largest release was estimated to have occurred during the first few days after the earthquake, including 15 March when the release rate was considered to have reached its maximum. Release rates were estimated to vary with time during March 2011, although these estimates have a large associated uncertainty because of the limited number of environmental data available as well as insufficient information on reactor conditions.

In this study, we attempt to estimate the temporal change in the release rate of I-131 and Cs-137 from environmental monitoring data using atmospheric

*Corresponding author. Email: s-hirao@ees.nagoya-u.ac.jp

transport simulations. The principle of the source-term estimation is similar to the inverse estimation method used in previous studies [1]. This method largely relied upon atmospheric concentration data obtained unequally in time and space in a relatively small area of approximately 60 km from the accident site, except for the atmospheric concentration data obtained in Ibaraki, which was approximately 100 km to the south of the FDNPP. It was noted in our former study [10] that the estimation of the source term from environmental monitoring data obtained within a short distance is difficult. This is because the release rate estimation is very sensitive to errors in the meteorological field, especially in wind direction, used in the atmospheric transport simulations. The release rate estimation published by the Tokyo Electric Power Company (TEPCO) [9] might suffer serious error for this reason. Conversely, using monitoring data obtained at a greater distance, such as atmospheric concentration data obtained predominantly on the North American continent [2], usually yields more robust estimations of source terms [11–13]. However, estimations from distant data might subject to greater uncertainty in the deposition process modeling than when local data are used. From these considerations, we decided to use environmental monitoring data predominantly by monitoring points in the regional area (i.e. at a distance of one to several hundred kilometers), for which atmospheric transport simulations are not subject to serious errors in both wind direction and deposition. Since more data are available in the regional area than in the local area, it is also intended in this study to evaluate the uncertainty in the estimated release rate.

2. Methodology and calculations

2.1. Release rate estimation

The estimation of the release rate is based on the principle that the atmospheric dispersion model can calculate a spatial distribution of relative values for the air concentration and deposition rate on the ground while their absolute values are unknown [10]. According to this principle, the ratio of air concentration and deposition rate to the release rate can be assumed to be the same for both measurements and calculations as follows:

$$\left(\frac{Q_r}{S_r}\right)_{t,i} = \left(\frac{Q_m}{S_m}\right)_{t,i} \quad (1)$$

where S_m is the release rate used for model calculations, Q_r is the measured air concentration or the measured deposition rate, Q_m is the calculated atmospheric concentration or the calculated deposition rate. The subscripts t and i denote the sampling time and sampling point, respectively.

In this study, we tried to estimate the release rate for every 3 h period. An observed air concentration or deposition used in this analysis represents a sampling duration of certain length, e.g. typically 24 h for the deposition data, to which release during multiple 3 h periods might have contributed. Therefore, the sum of the contributions calculated with an assumption of constant release rate was used to calculate the numerator of the right-hand-side of Equation (1) to result in a single value of estimated release rate from the single value of observation. The estimated release rate was assigned to the period that contributed the observed value. With this procedure, a 3 h-long release period might be assigned none, one, or multiple values of the estimated release rate. There might be more than two different release rate values estimated from independent monitoring data. In this case, a geometrical mean was applied to estimate a single value for the time and a geometrical standard deviation was calculated to estimate the uncertainties of the estimated values.

2.2. Environmental monitoring data

For the estimation of the release rate, the air concentrations and deposition rates of I-131 and Cs-137 were used; **Table 1** summarizes the sampling points and the number of data. The air concentrations were measured by the Japan Chemical Analysis Center (JCAC) in Chiba [14], Japan Atomic Energy Agency (JAEA) in Tokai [15], and High Energy Accelerator Research Organization and the National Institute for Environmental Industrial Technology Research Institute (KEK-NIES) in Tsukuba [16]. Air concentrations were measured using dust samplers with glass fiber filters and charcoal filters for particulate and gaseous species, respectively. The deposition rates on the

Table 1. List of sampling points for air concentration and deposition rate used in this study.

Sampling points	Prefectures	Source	Number*
Atmospheric concentration			
Tokai	Ibaraki	JAEA	30
Tsukuba	Ibaraki	KEK-NIES	12
Chiba	Chiba	JCAC	12
Deposition rate			
Yamagata	Yamagata	MEXT	6
Tokai	Ibaraki	JAEA	10
Hitachinaka	Ibaraki	MEXT	6
Utsunomiya	Tochigi	MEXT	4
Maebashi	Gunma	MEXT	2
Saitama	Saitama	MEXT	6
Chiba	Chiba	JCAC	12
Ichihara	Chiba	MEXT	6
Shinjuku	Tokyo	MEXT	6
Chigasaki	Kanagawa	MEXT	4
Total			116

Note: *This gives the number of valid measurements of I-131 and Cs-137 used for the release rate estimation.

ground were measured by the JCAC, JAEA, and Ministry of Education, Culture, Sports, Science and Technology (MEXT) at each Japanese prefecture [17]. The duration of the sampling periods ranged from less than 1 h to 40 h. The MEXT data are available for daily depositions of I-131 and Cs-137 from 18 March 2011. Of all the prefectures, the measurement data at Chiba, Gunma, Ibaraki, Kanagawa, Tochigi, Tokyo, Saitama, and Yamagata were used.

To eliminate the influence of resuspended radionuclides, the following criteria were set for the data selection: (1) the air concentration of Cs-137 to be greater than 0.01 Bq m^{-3} for Chiba and Tsukuba, and 0.3 Bq m^{-3} for Tokai, (2) the deposition rate of Cs-137 to be greater than 1.0×10^2 Bq m^{-2} day^{-1} for all deposition data. The air concentrations and deposition rates of I-131 at the sampling points and sampling times meeting the criteria for Cs-137 were used. Monitoring data that detected the radioactive plume that had passed over the ocean for more than 12 h were not used in our analysis to reduce uncertainties in the atmospheric dispersion model associated with longer simulation periods. Altogether, 54 air concentrations of Cs-137 and I-131 and 62 deposition rates of Cs-137 and I-131 were used in this study.

2.3. *Atmospheric dispersion model*

A Lagrangian particle random-walk model (LPRM) [10] coupled with a non-hydrostatic atmospheric dynamic model MM5 [18] was used to calculate the dispersion of the radioactive plume released from FDNPP. MM5 calculates the three-dimensional wind field and vertical diffusion coefficient. Radioactive decay, dry deposition, and wet deposition were calculated using LPRM. The LPRM calculates the movement of particles representing radionuclides by temporally and spatially varying meteorological fields. Cs-137 and I-131 were modeled as passive tracers by radioactive decay, with half-lives of 30 years and 8.04 days, respectively.

Dry and wet depositions were represented in the model simply by a deposition velocity and a scavenging coefficient, respectively. The deposition velocity was set to be 1.0×10^{-3} m s^{-1} and the scavenging coefficient was expressed as $8.0 \times 10^{-5} (I/I_0)^{0.8}$ s^{-1}, where I is the precipitation intensity and $I_0 = 1.0$ mm h^{-1} [19,20]. Although it has been noted that the deposition velocity and scavenging coefficient vary depending on the physicochemical characteristics of the nuclides, the above-mentioned constant values were used. This is because the measured data of the gas-particle partitioning and particle-size distribution are still very limited.

2.4. *Calculation conditions*

The calculation domain of the atmospheric dispersion model is shown as domain 2 in **Figure 1**. The

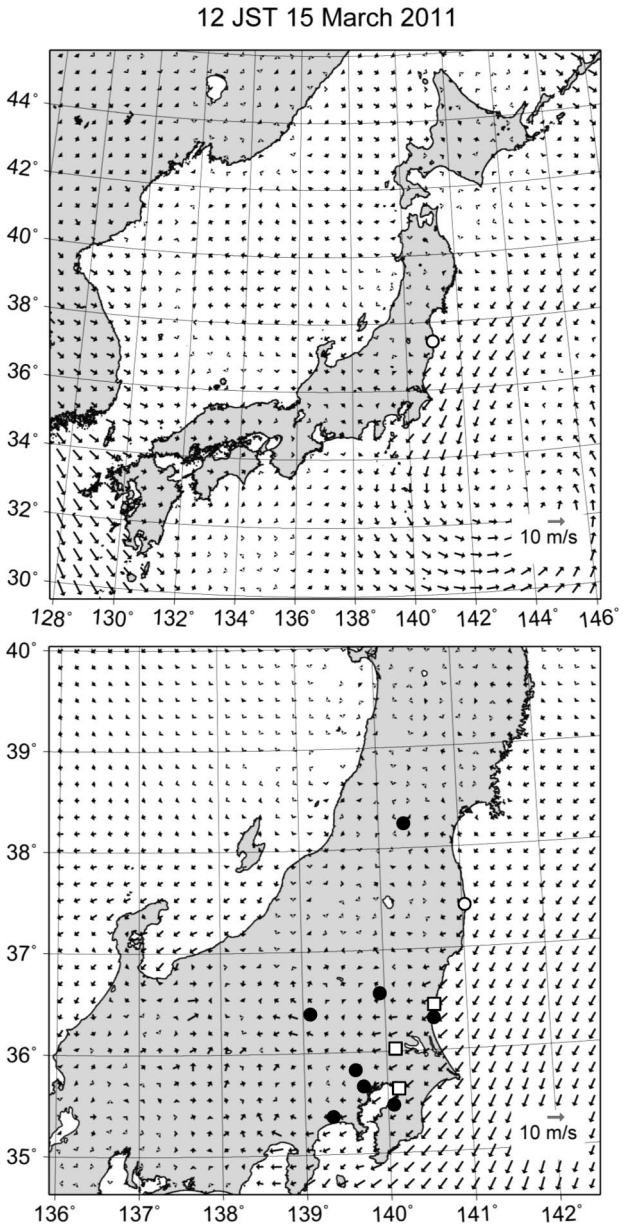

Figure 1. Map of the calculation domain 1 (upper) and domain 2 (bottom) used in the atmospheric dispersion model. The open circle shows the location of FDNPP. The black circles represent the monitoring points for deposition rate and the open squares represent monitoring points for air concentration and deposition rate.

domain covers most of the eastern part of the Honshu Island. **Table 2** shows the parameters used in the atmospheric dispersion model calculation. **Table 3** summarizes other specifications and physical processes of MM5 used in this work.

For initial and boundary conditions and the four-dimensional data assimilation of the meteorological fields in domain 1, the JRA-25 reanalysis data provided by the Japan Meteorological Agency (JMA) and the Central Research Institute of Electric Power Industry (CRIEPI) [21] were used. Topography and land-use data were obtained from the United States Geological

Table 2. Calculation conditions for the atmospheric dispersion model (domain 2).

Parameter	Value
Horizontal grid number	300 × 300
Grid size	2 km
Number of layers	25
Top	6 km
Time step	5 s

Note: The vertical z*-coordinate is defined as 10, 20, 30, 40, 50, 60, 70, 80, 90, 100, 150, 200, 400, 600, 800, 1000, 1500, 2000, 2500, 3000, 3500, 4000, 4500, 5000, 6000.

Table 3. Domain specification and physical schemes for the meteorological model MM5.

Scheme	Domain 1	Domain 2
Horizontal coordinate	Lambert conformal	
Vertical coordinate	Terrain-following sigma-coordinate	
Horizontal grid number	100 × 100	100 × 100
Horizontal grid size	18 km	6 km
Time step	50 s	16.667 s
Number of layers	30	
Top level	100 hPa	
Cumulus parameterization	Kain–Fritsch	None
Planetary boundary layer scheme	Gayno-Seaman PBL	
Explicit moisture scheme	Reisner graupel (Reisner 2)	
Radiation scheme	RRTM longwave scheme	
Surface scheme	Five-Layer Soil model	
Nesting	One-way nest	

Note: The vertical sigma-coordinate is defined as 1.00, 0.9975, 0.995, 0.990, 0.985, 0.980, 0.975, 0.970, 0.96, 0.95, 0.94, 0.93, 0.92, 0.91, 0.90, 0.89, 0.87, 0.86, 0.85, 0.80, 0.75, 0.70, 0.65, 0.60, 0.55, 0.50, 0.40, 0.30, 0.20, 0.10 and 0.00.

Survey global database. The radar-AMeDAS precipitation analysis data from JMA were used for the precipitation intensity in the wet deposition calculation.

The MM5 calculation was conducted for the period from 09 JST, 8 March to 00 JST, 1 April. The first two days of the calculation period were the spin-up time to properly simulate meteorological fields. The dispersion of I-131 and Cs-137 from FDNPP started at 05 JST, 12 March and ended at 00 JST, 1 April. The release height was set to be 15 m above the ground. A constant release rate of 1 TBq h^{-1} was assumed.

3. Results and discussion

The release rates of I-131 and Cs-137 were estimated for every 3-h time segment on March 2011. **Figure 2** shows the estimated temporal change in release rates with geometric standard deviations. The

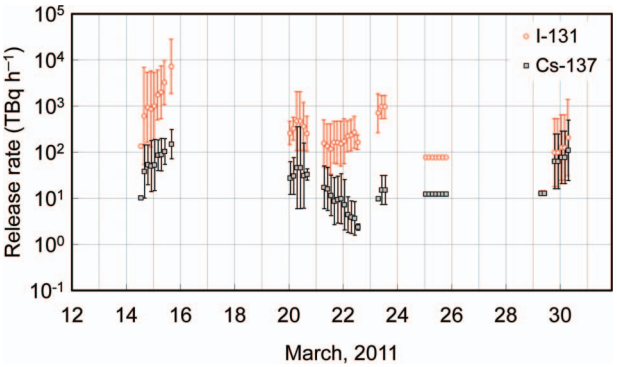

Figure 2. Estimated temporal change in release rate of I-131 and Cs-137 every 3-h time segment. Vertical bars represent geometric standard deviations of release rate. The red open squares represent the estimated release rates of I-131 and the gray squares represent the ones of Cs-137.

release rates were estimated on 14, 15, 20–23, 25, 29, and 30 March. The release rate could not be estimated for the period during which there was no environmental monitoring data that detected the radioactive plume. The geometric standard deviation could not be calculated for the time segments in which only one monitoring datum was available.

According to the present results, the release rates increased substantially from the afternoon of 14 March to the next afternoon, reaching a maximum release rate of 7.2×10^{15} Bq h^{-1} for I-131 and 1.5×10^{14} Bq h^{-1} for Cs-137 at 15–18 JST. After this maximum, the release rate was not estimated for subsequent four days. The release rate of I-131 was estimated to be $(2.5–4.7) \times 10^{14}$ Bq h^{-1} for 20 March, which is approximately 20 times smaller than the maximum, and to maintain values in the range of $(1.2–2.7) \times 10^{14}$ Bq h^{-1} during the following few days. A substantial decrease in the release rate during the period 15–19 March was also found for Cs-137, but the decrease is not as large as that of I-131. The Cs-137 release rate for 20 March was $(2.7–4.6) \times 10^{13}$ Bq h^{-1}, decreasing to 2.4×10^{12} Bq h^{-1} by a factor of approximately 10 over the following days. The release rates on 23 March were 9.6×10^{14} Bq h^{-1} and 1.7×10^{13} Bq h^{-1} for I-131 and Cs-137, respectively, and a significant increase in release must have occurred during the period from the afternoon of 22 March to the morning of March 23 to reach values of 9.6×10^{14} Bq h^{-1} and 1.7×10^{13} Bq h^{-1} for I-131 and Cs-137, respectively. The release rate estimated for 25 March implies that the release of I-131 decreased significantly while that of Cs-137 remained unchanged. Although the release rates for the period from 26 to 28 March are unknown, a slight increase on 29 and 30 March was indicated for both the nuclides. The increase was more enhanced for Cs-137.

Figure 3 shows the ratio of the estimated release rate of I-131 to that of Cs-137. The ratio increased from 13 to 49 from 14 to 15 March. The ratio was

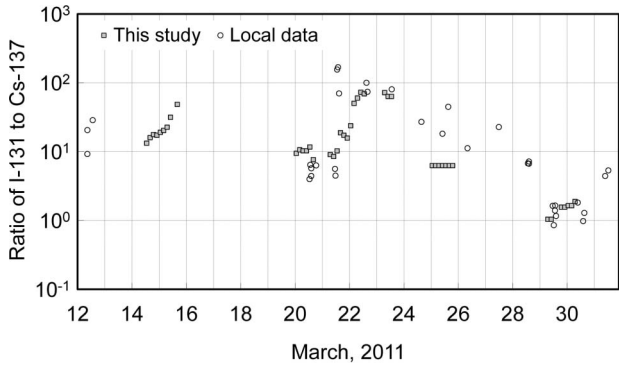

Figure 3. Temporal change in the ratio of the estimated release rate of I-131 to that of Cs-137 every 3-h time segment compared with the ratio calculated from the measured air concentration taken in the local area around FDNPP. The gray squares represent the estimated ratios from this study and the open circles represent the ones from the measured air concentration.

rather constant, at approximately 10, from the morning of 20 March to the afternoon of 21 March, and then increased to 70 at 09 JST, 22 March. At the end of March, the ratio of I-131 to Cs-137 was in the range of 1–2. The temporal change in the ratio estimated in this study was compared with the ratio for the air concentrations sampled on land near FDNPP [22,23], on sea offshore Fukushima [24], and at a height of approximately 3000 m offshore Fukushima [25]. The ratio for the local data was in the range of 4–6 from the morning of 20 March to the afternoon of 21 March, and then increased significantly at 13 JST, 21 March. The ratio from 22 to 29 March decreased substantially with an effective half-life of approximately 1.3 days, smaller than that of 8.02 days for I-131. The ratio on 30 and 31 March varied within the range 1–5. Both temporal changes are in good agreement, supporting the rapid increase of the ratio on 21 and 22 March.

3.1. *Uncertainty of estimated release rate*

To evaluate the uncertainty of the estimated release rate, the ratio of the estimated value S_i^t at i -th monitoring data to the geometric mean $\bar{S}^t$ of the time segment t was used as follows:

$$R_i^t = \frac{S_i^t}{\bar{S}^t}. \quad (2)$$

If the estimated release rates for a certain time are consistent, as is the case where the estimated release rates have the same values for all monitoring data, the ratio R^t becomes one. Therefore, this parameter would be a good measure of the uncertainty of the release rate estimated for each time segment.

Figure 4 shows the frequency distribution of the ratio R^t for all time segments and for all monitoring data. The total numbers of the population were 302. The values of R^t were in the range from 2.9×10^{-2} to 4.0×10^{1} for I-131 and 8.4×10^{-2} to 4.7×10^{1} for Cs-137. The geometric standard deviations were obtained as 3.3 and 2.9 for I-131 and Cs-137, respectively. This indicates that the uncertainty in the estimated release rate is a factor of approximately three.

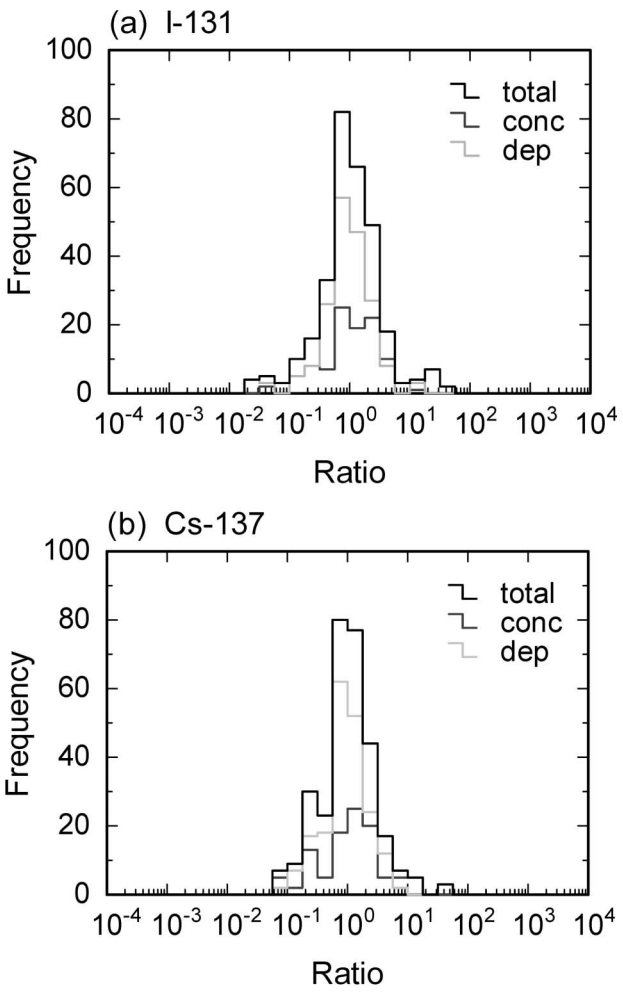

Figure 4. Frequency distribution of the ratios of the release rate to the geometric mean: (a) I-131, (b) Cs-137. Gray lines represent the results from the atmospheric concentrations, light-gray lines represent the results from the deposition rate, and black lines represent the results from both.

The geometric means of R^t for the air concentration were 1.2 and 1.3 for I-131 and Cs-137, respectively. The values of R^t for the deposition rate were 0.91 and 0.87 for I-131 and Cs-137, respectively. This suggests a small systematic difference of the estimated release rates between the values estimated from the air concentration and deposition rate.

The main sources of the uncertainties might be the errors in the wind field calculated using a meteorological model and the uncertainties of the modeling of the deposition processes characterized by the

deposition velocity and scavenging coefficient. In the present estimation, the release rate in one time segment was obtained by several pairs of measured-and-calculated air concentration and deposition rates. The uncertainty of this value was estimated to be a factor of approximately three; smaller than the uncertainty expected to be introduced by errors in the wind field. For instance, a few degrees of error in wind direction will cause an error in the calculated air concentrations in a plume of several orders of magnitude, and hence the significant error in the estimated release rate. This is enhanced at the edge of the plume. Therefore, the smaller uncertainty suggests that the spatial distribution patterns of plumes and depositions are reasonably calculated using the wind field calculated using MM5. The estimated release rate is not seriously influenced by the errors in the wind field.

One possible explanation for the systematic difference of the estimated release rates between the values estimated from the air concentration and deposition rate is the errors in the deposition parameters of the deposition velocity and the scavenging coefficient. If these parameters are assumed to be larger in the atmospheric dispersion model than in the actual conditions, the calculated air concentration becomes smaller and the calculated deposition rate increases. On the basis of these calculated values, a systematic difference occurs. In addition, the large deposition parameters could result in both the smaller calculated values of the air concentration and deposition rate as well as the systematic difference. This means that the release rate might be estimated to be systematically larger. In the following section, the temporal change in the estimated release rate is shown to be in good agreement with the release rates obtained by other researchers. This consistency suggests that errors in the assumed deposition parameters do not cause a serious overestimation of the release rate.

3.2. 15 March

We found that the estimated release rates at 09–12 JST and 15–18 JST, 15 March have a large uncertainty for the following reasons. First, the release rates during these periods were estimated from pairs of measured-and-calculated air concentration and deposition rate at the one monitoring point in Tokai in the early morning of 16 March. The radioactive plume released during 09–18 JST, 15 March was calculated to reach Tokai after flowing to northwest of FDNPP. Therefore, it took a long time for the plume to reach the monitoring point after release. Second, there was rain in Fukushima prefecture on the night of 15 March. The errors in the calculated air concentration and deposition rate become larger with the increase in the travel time of the plume in the atmosphere. This is because the calculated air concentration and deposition rate of the plume over long travel times are influenced by both errors in the wind field and modeling of removal processes for long periods of time. In addition, the difference of the scavenging coefficient between in-cloud deposition and below-cloud deposition is not taken into account in the atmospheric dispersion model for reasons of simplicity. Therefore, the estimated release rates at 09–12 JST and 15–18 JST, 15 March is concluded to have a larger uncertainty than the other values estimated by the plume that was transported in a shorter travel time and over no rain area.

3.3. 19 and 20 March

It was noted that the release rate on 19 and 20 March is probably larger than the estimated release rate for 20 March mentioned above. In the present estimation, we excluded the pairs of the measured-and-calculated air concentration and deposition rate affected by the plume with a long travel time over the ocean. The excluded monitoring data were the air concentrations in Tokai and Chiba, and the deposition rate in Ibaraki, Chiba, Tokyo, Saitama, Tochigi, Kanagawa, and Gunma from the morning of 20 March to the next morning, and the deposition rates in Ibaraki from the morning of 25 March to the next morning. If these data are used for the estimation, the release rates from the night of 19 March to the next morning and at midnight of 25 March are estimated to be larger than the original estimated values as shown in **Figure 5**. Their geometric standard deviations are also estimated to be large. The uncertainty in the estimated release rate might be enhanced by using the concentration of and deposition from plumes with the long travel times. The plume discharged in the early afternoon of 19 March reached the Kanto region in the next morning after once travelling over the Pacific Ocean for approximately 12 h. During this period, the plume did not experience rain and the dry deposition process was dominant. Since the dry deposition velocity of 1.0×10^{-3} m s^{-1} used in the model calculation,

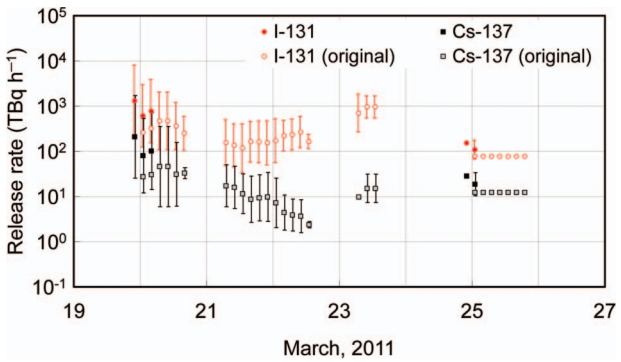

Figure 5. Estimated temporal change in the release rate of I-131 and Cs-137 using the monitoring data affected by the radioactive plume at prolonged travel times over the ocean. Open circles and solid gray squares mean the same as described for Figure 2.

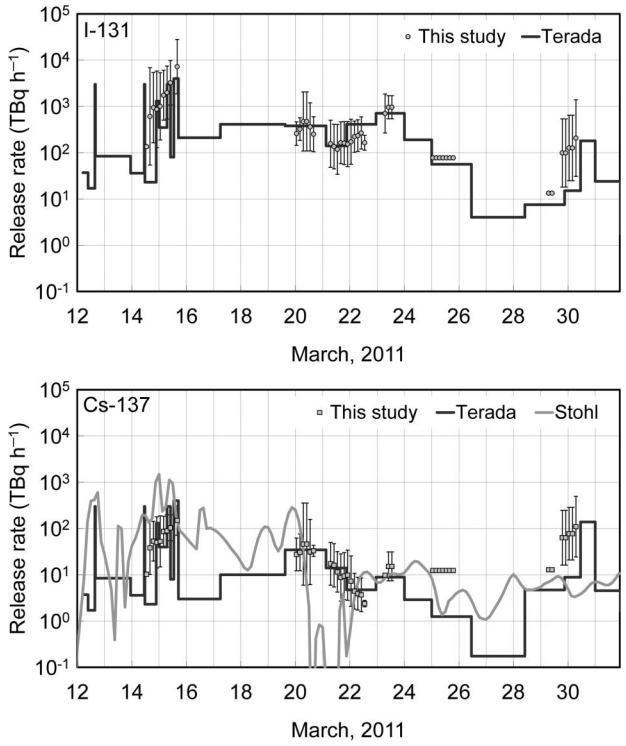

Figure 6. Comparison of the estimated temporal changes in the release rate of I-131 and Cs-137. Black solid line, Terada et al. [8]; gray solid line, Stohl et al. [2].

which is a typical value for the land surfaces, was probably too large for sea surfaces, the calculated depletion of the plume due to dry deposition during the travel over the ocean might have caused underestimation of the air concentration and deposition to cause overestimation of the release rate. The plume was further transported toward inland of Kanto Plains on 20 March until it encountered precipitation in the early morning of the next day causing wet depositions at the monitoring points, which were also used in the present analysis. This long travel time of plume for more than 24 h might have caused errors in the transport–deposition calculations. This is also a source of uncertainty in the release rate estimated from these monitoring data. However, we cannot ignore the possibility of the large release rate on 19 and 20 March.

4. Comparison with former estimations

In **Figure 6**, the estimated release rate was compared to the results of Terada et al. [8] and Stohl et al. [2]. Our result shows good agreement with both results within the limits of uncertainty. The significant release during 14 and 15 March, the trend in the middle of March, and the temporal increase at the end of March are common to all previous estimations except for the significant underestimate of Cs-137 release for 20–22 March by Stohl et al. [2]. This agreement despite the use of different sets of monitoring data supports the reliability of the estimated temporal changes. In this study, to estimate the total amount of the atmospheric release during March 2011, the release rate by Terada et al. [8] was inserted into the period in which the release rates were not estimated. The total amounts of I-131 and Cs-137 estimated were compared with the results of Terada et al. [8] and Stohl et al. [2] in **Table 4**. The total amount of release until 31 March was estimated to be 1.5×10^{17} Bq for I-131 and 9.6×10^{15} Bq for Cs-137, which was slightly higher than the result of 1.2×10^{17} Bq for I-131 and 8.6×10^{15} Bq for Cs-137 estimated by Terada et al. [8]. This difference for I-131 resulted mainly from the larger release rate on 15 March than Terada et al.'s [8] estimation. For Cs-137, the difference came from the sum of the differences in the release rate on 15, 25, 29, and 30 March. The total amount of release of Cs-137 estimated by Stohl et al. [2] is significantly larger than our value. This is caused by the larger release rates than our estimates in the early phase of the accident. This difference from our estimated release rate came from the inverse modeling method applied by Stohl et al. [2], which is likely to be constrained strongly to the a priori estimate of release rate, and from the assimilated observation data sampled at distant places in the northern Hemisphere.

Table 4. Comparison of the estimated release amount of I-131 and Cs-137.

	Until 31 March		14–15 March	
	I-131 (Bq)	Cs-137 (Bq)	I-131 (Bq)	Cs-137 (Bq)
Present study	1.5×10^{17}	9.6×10^{15}	6.5×10^{16}	2.9×10^{15}
Terada et al. [8]	1.2×10^{17}	8.6×10^{15}	3.5×10^{16}	3.4×10^{15}
Stohl et al. [2]		3.6×10^{16}		1.9×10^{16}

5. Conclusion

We have estimated the release rates of I-131 and Cs-137 from the FDNPP and their uncertainties with a 3-h temporal resolution in March 2011. The release rate estimation is based on a simple inverse method by combining the environmental monitoring data that are available to the research community and regional range atmospheric dispersion calculations. The release rates were estimated only for some specific days of March and not for the entire month, because the land-based environmental monitoring in the region did not detect all of the radioactive plumes. Despite this limitation, the temporal change in the release rates was reasonably well estimated and their uncertainties were evaluated to be a factor of 3.3 for I-131 and 2.9 for Cs-137. A large release was estimated to have started on the night of 14 March and continued at least

until the afternoon of 15 March. Maximum release rates of 7.2×10^{15} Bq h^{-1} for I-131 and 1.5×10^{14} Bq h^{-1} for Cs-137 were obtained. The release rate on 20–23 March changed in the range $(1.2–9.6) \times 10^{14}$ Bq h^{-1} for I-131 and $(0.24–4.6) \times 10^{13}$ Bq h^{-1} for Cs-137. A slight increase in the rate for both nuclides was estimated on 29 and 30 March. The estimated release rate indicates that the release of I-131 decreased during March while that of Cs-137 remained unchanged.

The uncertainty in the estimated release rates in the afternoon of 15 March and in the early morning of 20 March is larger than that in other periods. The uncertainties of the estimated release rate might be enhanced because of errors in the removal process calculations in cases where the travel time of the plume transported from the FDNPP to the monitoring points was prolonged. For further discussion, it is necessary to analyze the sensitivities of the release rate estimations to different deposition parameters and deposition schemes. An optimization of the deposition parameters could help to estimate release rates with less uncertainty.

Acknowledgements

This work was partly supported by JSPS KAKENHI grant number 24110002. We would like to thank JMA and CRIEPI for the JRA-25/JCDAS dataset.

References

[1] Chino M, Nakayama H, Nagai H, Terada H, Katata G, Yamazawa H. Preliminary estimation of release amounts of ^{131}I and ^{137}Cs accidentally discharged from the Fukushima Daiichi nuclear power plant into the atmosphere. J. Nucl. Sci. Technol. 2011;48:1129–1134.

[2] Stohl A, Seibert P, Wotawa G, Arnold D, Burkhart JF, Eckhardt S, Tapia C, Vargas A, Yasunari, TJ. Xenon-133 and caesium-137 releases into the atmosphere from the Fukushima Dai-ichi nuclear power plant: determination of the source term, atmospheric dispersion, and deposition. Atmos. Chem. Phys. 2012;12:2313–2343.

[3] Katata G, Ota M, Terada H, Chino M, Nagai H. Atmospheric discharge and dispersion of radionuclides during the Fukushima Dai-ichi nuclear power plant accident. Part I. Source term estimation and local-scale atmospheric dispersion in early phase of the accident. J. Environ. Radioact. 2012;109:103–113.

[4] Katata G, Terada H, Nagai H, Chino M. Numerical reconstruction of high dose rate zones due to the Fukushima Dai-ichi nuclear power plant accident. J. Environ. Radioact. 2012;111:2–12.

[5] NISA, Nuclear and Industrial Safety Agency [Internet] [cited 2012 Oct 15]. Available from: http://www.nsr.go.jp/archive/nisa/english/files/en20110412-4.pdf.

[6] NISA, Nuclear and Industrial Safety Agency [Internet] [cited 2012 Oct 15]. Available from: http://www.nsr.go.jp/archive/nisa/english/press/2011/06/en20110615-5.pdf.

[7] Winiarek V, Bocquet M, Saunier O, Mathieu A. Estimation of errors in the inverse modeling of accidental release of atmospheric pollutant: application to the reconstruction of the cesium-137 and iodine-131 source terms from the Fukushima Daiichi power plant. J. Geophys. Res. 2012;117:D05122.

[8] Terada H, Katata G, Chino M, Nagai, H. Atmospheric discharge and dispersion of radionuclides during the Fukushima Dai-ichi nuclear power plant accident. Part II. Verification of the source term and analysis of regional-scale atmospheric dispersion. J. Environ. Radioact. 2012;112:141–154.

[9] TEPCO, Tokyo Electric Power Company [Internet]. [cited 2012 Aug 1]. Available from: http://www.tepco.co.jp/en/press/corp-com/release/betu12_e/images/120524e0205.pdf.

[10] Hirao S, Yamazawa H. Release rate estimation of radioactive noble gases in the criticality accident at Tokai-Mura from off-site monitoring data. J. Nucl. Sci. Technol. 2010;47:20–30.

[11] Yamazawa H. Source term estimation method using long-range inverse atmospheric transport simulation. J. Atom. Energ. Soc. Jpn. 1998;40:885–891. [in Japanese].

[12] Yamazawa H. Long-range dispersion analysis on accidental atmospheric release of cesium-137 at Algeciras. J. Atom. Energ. Soc. Jpn. 1999;41:114–116. [in Japanese].

[13] Furuno A, Chino M, Yamazawa H. Development of a source term estimation method for nuclear emergency by long-range atmospheric dispersion simulations. J. Atom. Energ. Soc. Jpn. 2006;5:229–240. [in Japanese].

[14] Amano H, Akiyama M, Chunlei Bi, Kawamura T, Kishimoto T, Kuroda T, Muroi T, Odaira T, Ohta Y, Takeda K, Watanabe Y, Morimoto T. Radiation measurements in the Chiba metropolitan area and radiological aspects of fallout from the Fukushima Dai-ichi nuclear power plants accident. J. Environ. Radioact. 2012;111:42–52.

[15] Furuta S, Sumiya S, Watanabe H, Nakano M, Imaizumi K, Takeyasu M, Nakada A, Fujita H, Mizutani T, Morisawa M, Kokubun Y, Kono T, Nagaoka M, Yokoyama H, Hokama T, Isozaki T, Nemoto M, Hiyama Y, Onuma T, Kato C, Kurachi T. Results of the environmental radiation monitoring following the accident at the Fukushima Daiichi nuclear power plant – interim report (ambient radiation dose rate, radioactivity concentration in the air and radioactivity concentration in the fallout). JAEA Rev. 2011;2011–2035: 89p [in Japanese].

[16] KEK-NIES, high energy accelerator research organization, KEK, and National Institute for Environmental Studies [Internet]. [cited 2012 Aug 1]. Available from: http://www.kek.jp/ja/Research/ARL/RSC/Radmonitor/.

[17] MEXT, Ministry of Education, Culture, Sports, Science and Technology [Internet]. [cited 2012 Aug 1]. Available from: http://radioactivity.mext.go.jp/en/list/194/list-201103.html.

[18] Grell GA, Dudhida J, Stauffer DR. A description of the fifth-generation Penn State/NCAR Mesoscale Model (MM5). NCAR Tech. Note NCAR/TN-389 +STR. National Center for Atmospheric Research (NCAR), vol. 117; 1994.

[19] Baklanov A, Sørensen JH. Parameterisation of radionuclide deposition in atmospheric long-range transport modelling. Phys. Chem. Earth (B). 2001;26:787–799.

[20] Sportisse B. A review of parameterizations for modelling dry deposition and scavenging of radionuclides. Atmos. Environ. 2007;41:2683–2698.

[21] Onogi K, Tslttsui J, Koide H, Sakamoto M, Kobayashi S, Hatsushika H, Matsumoto T, Yamazaki N, Kamahori H, Takahashi K, Kadokura S, Wada K, Kato K, Oyama R, Ose T, Mannoji N, Taira R. The JRA-25 reanalysis. J. Meteor. Soc. Jpn. 2007;85:369–432.

[22] MEXT [Internet]. [cited 2012 Oct 15]. Available from: http://radioactivity.mext.go.jp/en/contents/4000/3156/24/115_hp_0912_18.pdf.

[23] NISA [Internet]. [cited 2012 Oct 15]. Available from: http://www.nsr.go.jp/archive/nisa/english/press/2011/06/en20110615-4.pdf.
[24] MEXT [Internet]. [cited 2012 Oct 15]. Available from: http://radioactivity.mext.go.jp/en/list/259/list-201103.html.
[25] MEXT [Internet]. [cited 2012 Oct 15]. Available from: http://radioactivity.mext.go.jp/en/list/234/list-1.html.